Pergamon

Journal of South American Earth Sciences, Vol. 11, No. 2, pp. 115–129, 1998

Printed in Great Britain

PII: S0895-9811(98)00005-4

0895-9811/98 $19.00 + 0.00

Source characteristics of historic earthquakes along the central Chile subduction zone

[1]S. BECK, [2]S. BARRIENTOS, [2]E. KAUSEL and [2]M. REYES

[1]SASO and Department of Geosciences, University of Arizona, Tucson, AZ 85721, U.S.A.
[2]Department of Geophysics, University of Chile, Santiago, Chile

Abstract — We have analyzed four large to great historic earthquakes that occurred along the central Chile subduction zone from north to south on November 11, 1922 ($M_s = 8.3$), April 6, 1943 ($M_s = 7.9$), December 1, 1928 ($M_s = 8.0$) and January 25, 1939 ($M_s = 7.8$). Waveform modeling and *P*-wave first motions indicate that the 1922, 1928 and 1943 earthquakes are shallow and consistent with underthrusting of the Nazca Plate beneath the South American plate. In contrast, the 1939 earthquake is not an underthrusting event but rather a normal fault event within the down-going slab.

The 1922 earthquake is by far the largest event with a complex source time function showing three pulses of moment release and a duration of 75 s. The 1943 earthquake has a simple source time function with one pulse of moment release and a duration of 24 s. This event had a local tsunami of 4 m and a far-field tsunami height in Japan of 10–30 cm. The 1928 earthquake also has a simple source time function with a duration of 28 s. The aftershocks and highest intensities are south of the epicenter indicating a southward rupture with most of the seismic moment release occurring 50–80 km south of the 1928 epicenter but still north of the adjacent 1939 earthquake region. The 1939 Chillan earthquake was not an underthrusting but rather a complex normal fault earthquake. Our preferred model is a normal fault mechanism at a depth of 80 to 100 km with two pulses of moment release and a total duration of approximately 60 s. The high intensities, lack of a tsunami, and inland location associated with the 1939 event are all consistent with an intraplate event within the down-going slab. The 1939 earthquake was clearly more destructive than the other similar size or larger events. This may in part be due to the intraplate nature of the event but also due to high amplification of the sites in the Central Valley of south central Chile. © 1998 Published by Elsevier Science Ltd. All rights reserved

Resumen — Se analizan cuatro grandes terremotos, ocurridos a lo largo de la zona de subducción en Chile central. Estos eventos sismicos, de norte a sur, son: Nov. 22, 1922, en Copiapó-Vallenar, Ms = 8.3; Abril 6, 1943 en Illapel-Combarbalá, Ms = 7.9; Dic. 1, 1928, en Talca, Ms = 8.0 y Enc. 25, 1939, en Chillán, Ms = 7.8.

Las formas de onda y polaridad del primer arribo de las ondas P a diferentes estaciones indican que el mecanismo focal de tres de estos terremotos es consistente con el fallamiento inverso de bajo ángulo producido por el desplazamiento de la placa de Nazca bajo la placa Sudamericana. Sin embargo, el terremoto de 1939 no presenta estas caracteristicas sino que es producto de un fallamiento normal que ocurre en el interior de la placa que subducta.

El terremoto de 1922 es, sin duda alguna, el evento más grande de esta serie. La función de tiempo en la fucntc es compleja, de 75 s de duración, y se compone de tres pulsos que representan diferentes etapas de liberación de momento. La deformación en el fondo oceánico asociada a este evento produjo como consecuencia un tsunami que alcanzó una altura de 7 m en la costa de la región epicentral (Caldera-Coquimbo), en tanto que en Japón alcanzó una altura de 30–70 cm. El evento de 1943 presenta una función de tiempo en la fuente relativamente simple que se compone de sólo un pulso de liberación de momento de 24 s de duración. El tsunami generado alcanzó localmente una altura de 4 m y 10–30 cn en Japón. Por otra parte, el terremoto de 1928 también presenta una función de tiempo simple, de 28 s de duración. Para este ultimo terremoto, tanto las réplicas como las mayores intensidades se localizan hacia el sur del epicentro indicando la existencia de un frente de ruptura que se propaga hacia el sur. La mayor liberación de momento se localiza a unos 50–80 km hacia el sur del inicio de la ruptura, pero aún fuera de la región involucrada en el terremoto de 1939. El tsunami producido fue del orden de 1 m frente a las costas de la región epicentral. Por otra parte, el terremoto de 1939 no ocurre sobre una falla inversa de bajo ángulo como los anteriores, sino que sobre una falla normal. Nuestra mejor solución corresponde a un fallamiento producto de un campo tensional, a unos 80–100 km de profundidad, con dos pulsos de liberación de momento y de una duración total cercana a los 60 s. Las altas intensidades, ausencia de tsunami y la localización epicentral hacia el interior del continente son consistenters con un evento intraplaca al interior de la placa que subducta. El evento de 1939 ha sido claramenta más destructivo que otros de tamaño similar o mayores. En parte, esto puede ser debido a las caracteristicas inherentes de los terremotos intraplaca como también a la mayor amplificación del movimiento del suelo en los valles del centro-sur de Chile. © 1998 Published by Elsevier Science Ltd. All rights reserved

INTRODUCTION

The subduction zone along the central coast of Chile has ruptured in large to great destructive earthquakes this century (Fig. 1, Table 1). Many, although not all, of these earthquakes are underthrusting events that represent the subduction of the Nazca plate beneath the South American plate. The historic earthquake record goes back well beyond this century and began around 1570 with the first accounts provided by Spanish settlers. A large number of earthquakes between 1570 and 1900 have been identified using intensity distributions, coastal movements, observed tsunamis, limits of perceptibility, and duration of

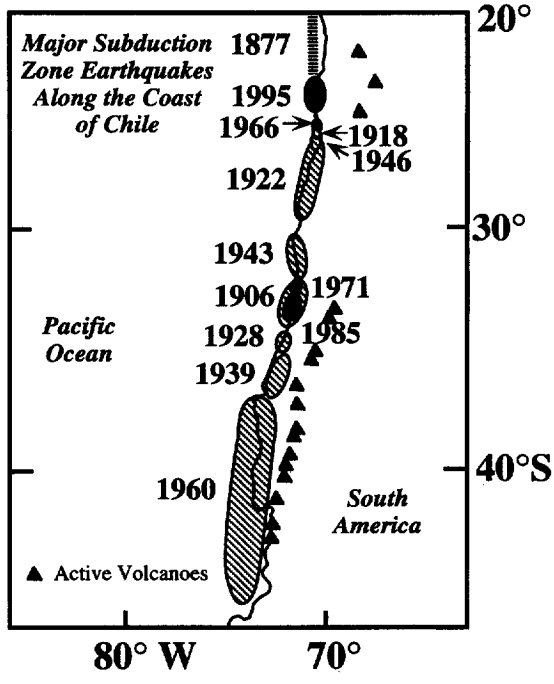

Fig. 1. Map of the largest earthquakes along the coast of Chile this century. The estimated rupture areas are from Kelleher (1972). Most but not all these earthquakes are underthrusting events associated with the subduction of the Nazca Plate beneath the South American Plate.

shaking (Fig. 2) (Willis, 1929; Heck, 1947; Berninghausen, 1962; Lomnitz, 1971; Kelleher, 1972; Nishenko, 1985). The long historic earthquake record and the large number of big events this century make the Chile subduction zone ideal for studying the earthquake cycle. In this study we focus on two segments of the Chile subduction zone from 26°S–32°S and 34°S–37.5°S where large earthquakes have occurred this century as well as historically.

The north central segment (between 26°S and 32°S) of Chile was the site of two great earthquakes this century, on earthquake on November 11, 1922 ($M_s = 8.3$) and the other on April 6, 1943 ($M_s = 7.9$). These earthquakes were damaging, particularly the 1922 event, which produced significant damage along more than 500 km of the coast (Willis, 1929).

The south central Chile segment (34°S to 37.5°S) has one of the most complete records of large earthquakes anywhere (Fig. 2). Two particularly devastating earthquakes occurred in adjacent segments along the coast of central Chile on January 25, 1939 ($M_s = 7.8$) and December 1, 1928 ($M_s = 8.0$) and were initially assumed to be underthrusting events for purposes of estimating seismic hazards. The 1928 earthquake devastated the cities of Talca and Constitucion and caused damage from Valparaiso to Concepcion (Fig. 3). Early reports showed an east–west trend of maximum intensities for the 1928 earthquake (Bobillier, 1939). Nishenko (1985) suggested that such an intensity pattern was more consistent with an intraplate event rather than an underthrusting event. The 1939 earthquake was one of the most destructive events to ever occur in Chile. This earthquake destroyed 90% of the city of Chillan and approximately 28,000 people died as a result of this event (Saita, 1840; Sarasola, 1939; Lomnitz, 1971). There was no report of a tsunami and the International Seismological Summary (ISS) gave this event a depth of 90 km. Campos and Kausel (1990) suggested that the 1939 earthquake was an intraplate normal event. This uncertainty in the mechanisms of the 1928 and 1939 events gives rise to a large range of probabilities (18–100%) for an underthrusting earthquake along this segment of the subduction zone in the next few decades (Nishenko, 1985, 1991). Nearly 80% of the population of Chile resides along or near this segment of the subduction zone, hence, it is extremely important to understand the range in fault types that can give rise to large damaging events.

We have collected and analyzed seismograms (primarily teleseismic *P* waveforms), intensity data, and tsunami information in order to characterize the source parameters for the 1922, 1943, 1928 and 1939 earthquakes.

DATA AND METHODS

Studying earthquakes prior to the installation of the WWSSN in 1963 is often difficult due to the sparse station coverage, the types of instruments, and the subsequent difficulty of retrieving old data. The useable instrumental data sets for earthquakes prior to 1963 are always sparse compared to modern data sets. However, even a sparse dataset can be very valuable for determining first order parameters about import-

Table 1. Large to great historic (1906 to 1955) earthquakes along the chile subduction zone

Earthquake m/d/y	Origin time h:min:s	Lat.	Long.	Mag.	Ref.
08/17/06	00:40:	33.0°S	72.0°W	M_s8.4	A&N
12/04/18	11:47:08	26.0°S	71.0°W	M_s7.6	Abe
11/11/22	04:32:06	28.5°S	70.0°W	M_s8.3	Abe
12/01/28	04:06:10	35.0°S	72.0°W	M_s8.0	Abe
01/25/39	03:32:14	36.25°S	72.25°W	M_s7.8	Abe
04/06/43	16:07:15	30.75°S	72.0°W	M_s7.9	Abe
08/02/46	19:18:48	26.5°S	70.5°W	M_s7.1	Abe
06/05/53	17:16:43	36.5°S	73.0°W	M_s7.6	Askew

This table is complete for $M > 7.6$ interplate earthquakes between 1906 and 1955 but is not complete for smaller earthquakes.
References for Magnitudes: A&N, Abe and Noguchi 1983; Abe 1981; Askew et al. 1985

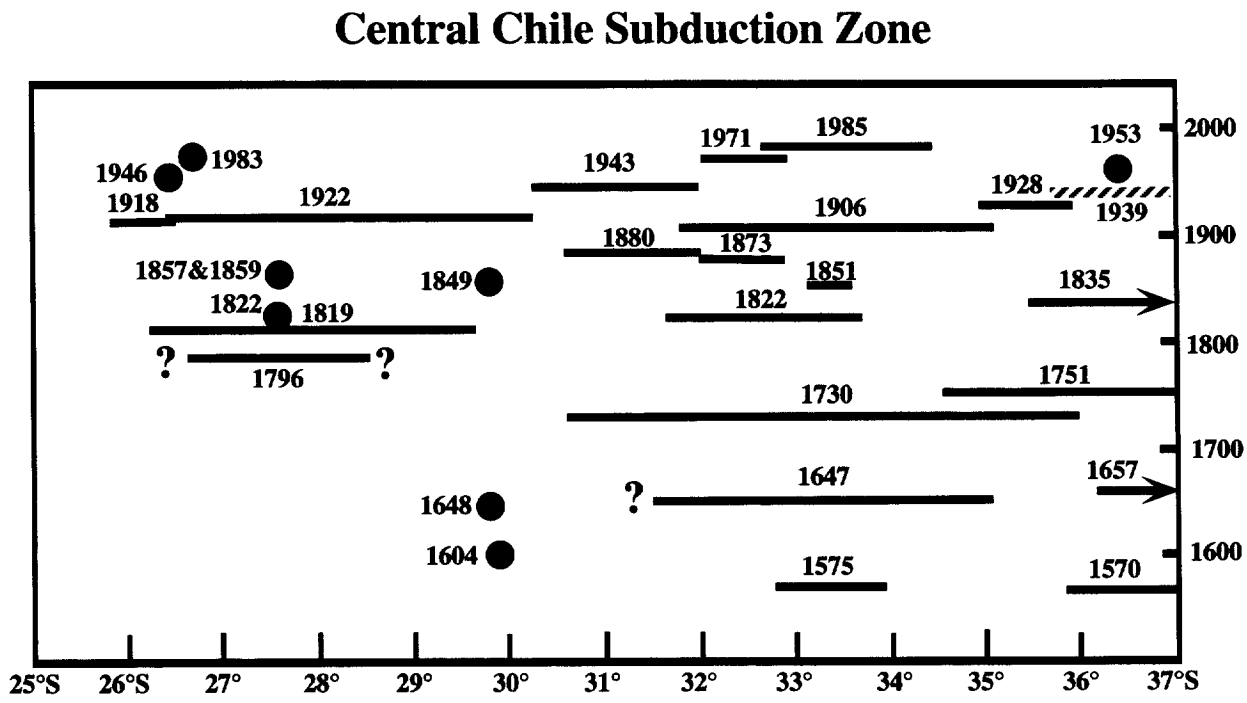

Fig. 2. Space-time plot of large to great earthquakes along the coast of south central Chile. Solid bars represent significant earthquakes that are probably underthrusting events. The length of the bar corresponds to the region of highest intensities and damage along the coast. The hatchured bar shows the location of the 1939 intraplate event. The solid circles represent smaller events that reported damage in one locality. The 1796 bar represents two events (March 30 and August 24) and the 1819 bar represents 3 events (April 3, 4, and 11). the earthquake size cut off is not uniform along the coast. Compiled from Lomnitz (1971), Willis (1929), Comte *et al.* (1986) and Askew and Algermissen (1985).

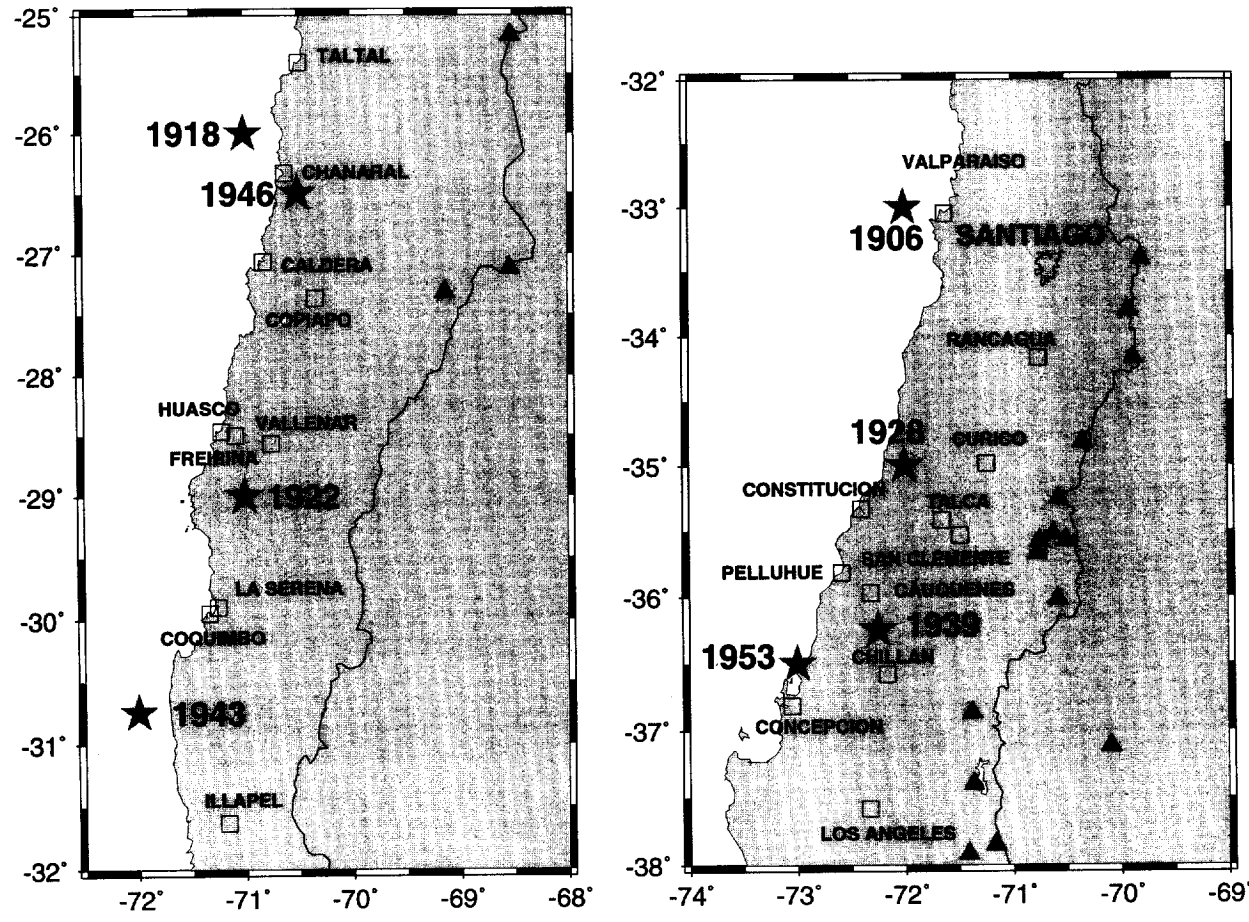

Fig. 3. Map showing the locations of the earthquakes in this study, and the cities and towns discussed in the text.

Table 2. Source parameters for large to great historic earthquakes along the chile subduction zone

Earthquake m/d/y	Origin time h:min:s	Strike (°)	Dip (°)	Slip (°)	M_w	Depth (km)	Duration (s)
11/11/22	04:32:06	0	20E	90	–	0–40	75
12/01/28	04:06:10	0	20–30E	90	7.8	0–25	24–28
01/25/39	03:32:14					80–100	60
04/06/43	16:07:15	0	20–30E	90	7.9	0–40	24

Strike dip and slip, moment magnitude and depth are determined in this study

ant earthquakes. We obtained seismograms and instrument responses from station operators throughout the world. We used as many records as possible to constrain the focal mechanism using first motions but only from records we obtained and could determine the polarity. The long-period seismograms from instruments such as the Galitzin, Benioff and in one case a modified Wood-Anderson were scanned and the *P* waves and in a few cases the *S* waves were digitized. We used both vertical and horizontal component *P* waves and diffracted *P* waves in order to increase the usable records.

We modeled the *P* waves using a multistation omnilinear inversion (Ruff 1989) and a single station inversion (Ruff and Kanamori 1983; Swenson and Beck 1996). Both methods invert for the source time function and seismic moment using an assumed focal mechanism and depth (or a distributed depth). The omnilinear inversion is ideal for historic seismograms because it simultaneously determines the source time function and trace scaling factors to minimize scatter in the amplitudes (Ruff, 1989). This allows us to use *P* waves with large uncertainties in the absolute amplitude. It is not always clear what the true magnification is for historic seismograms. For the largest events directivity due to large fault dimensions makes it difficult to simultaneously invert stations with very different ray parameters in the same inversion. Rarely is there enough station coverage to invert for a detailed slip distribution. Hence, we often restrict our multistation inversions to a few of the best records. We first constrain the focal mechanism as much as possible from *P*-wave first motions then use a grid search by varying the focal mechanism and depth to determine the best source parameters for each earthquake. We then determine the seismic moment from undiffracted vertical component *P* waves.Table 2

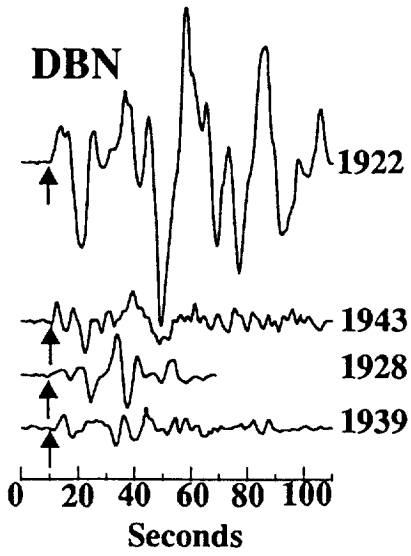

Fig. 4. Comparison of *P* waveforms recorded at DNB for the 1922 (Dist = 99°), 1943 (Dist = 101°), 1928 (Dist = 104°), and 1939 (Dist = 105°) earthquakes. The 1922 earthquake record has the largest amplitude and the longest duration.

NOVEMBER 11, 1922 ATACAMA EARTHQUAKE

The 1922 Atacama earthquake was one of the largest events to rupture the plate boundary this century. Figure 4 shows a comparison of the DBN record for the 1922 earthquake with other underthrusting events along the coast of Chile. The 1922 event is much larger, and has a much longer and more complex *P*

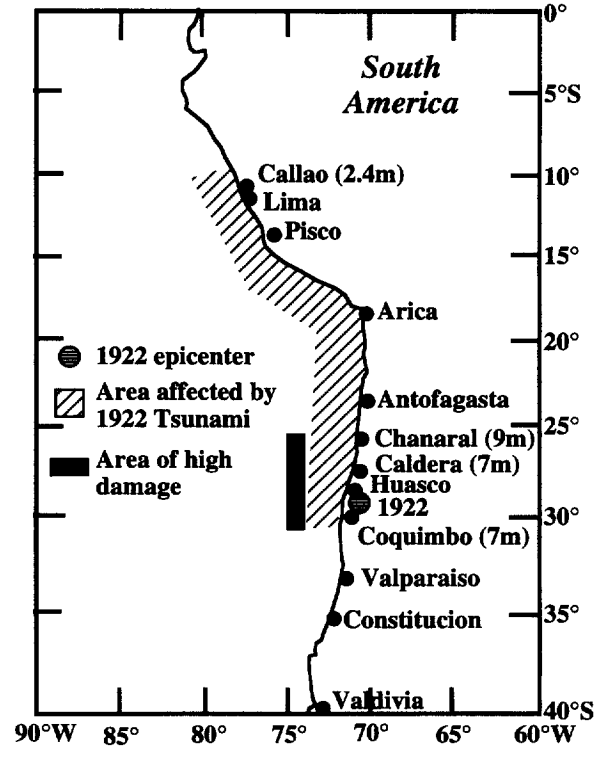

Fig. 5. Map of part of the west coast of South America showing the regions affected by strong damaging shaking and a tsunami generated by the November 11, 1922 earthquake. The coast from Coquimbo to Chanaral was significantly damaged during the 1922 earthquake. The tsunami affected the coast primarily north of the 1922 epicenter.

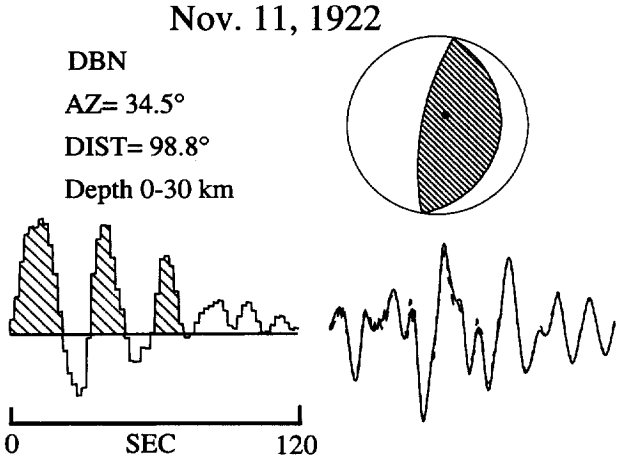

Fig. 6. Source time function for the November 11, 1922 earthquake determined from the P waveform recorded at DBN. The observed *P*-wave is the solid line and the synthetic waveform is the dashed line. Note the three major pulses of moment release with a total duration of 75 s. The focal mechanism is based on *P*-wave first motions.

waveform than the other events. The 1922 event generated a local tsunami along the coast with a maximum height of 9 m at Chanaral (Fig. 5) and a far field tsunami in Japan of 39–70 cm, suggesting an underthrusing mechanism (Willis, 1929; Lomnitz, 1971; Hatori, 1968). The S–P times of aftershocks reported at La Paz, Bolivia indicate an aftershock zone of approximately 470 km in the north–south direction (Kelleher, 1972). Although there were numerous seismic stations operating in 1922, few were long-period instruments ideal for body wave modeling, although many are useful for *P*-wave fist motions. We obtained seismograms to help constrain the *P*-wave first-motion mechanism for the 1922 earthquake and used only records with the instrument polarities indicated. All of the teleseismic *P*-waves show compressional first-motion arrivals, also indicative of an underthrusting earthquake.

The *P*-wave seismogram from station DBN (DeBilt) is high quality and hence, ideal for modeling. With one diffracted *P*-wave we cannot constrain the mechanism or the seismic moment. However, we can use this station to constrain the source duration and complexity. We fix the focal mechanism to be underthrusting, with the shallow plane striking parallel to the trench and dipping 20° to the east. We then invert the *P* wave from DBN for the source time function at a series of trial depths using the method of Ruff (1989). The depth is difficult to determine due to the long duration of the source and the trade off with the source time function. We assume that the earthquake is shallow (0–40 km), as are most underthrusting earthquakes along the coast of Chile. With these assumptions the source time function has a duration of at least 75 s, with three pulses of moment release (Fig. 6). The tsunami reports indicate that a significant tsunami occurred north of the 1922 epicenter all the way into Peru but there were no reports of a tsunamis to the south along the coast of Chile (Fig. 5). This, along with the damage reports suggest a primarily northward rupture for the 1922 earthquake. The 75 s durations suggests a minimum rupture length of 150–225 km (assuming an unilateral rupture velocity of 2–3 km/s).

Shortly after the 1922 earthquake, Baily Willis of the Carnegie Institute traveled to Chile to investigate the 1922 earthquake and, in particular, to find surface rupture (Willis, 1929). Although Willis never found any surface rupture, the result was a fascinating volume describing the earthquake damage, eye-witness accounts, tsunami heights, and local geology (Willis, 1929). Willis, along with Dr Luis Sierra, collected information about the local damage all along the coast. They received 300 of 1000 questionnaires that they sent out asking residents to describe the earthquake shaking and resulting damage. The damage and corresponding intensities were difficult to interpret because of the variability of local sites and construction practices. There was a large region of apparent high intensities. Willis was hoping to determine the epicenter based on the intensities but found that impossible because there was such a large area of high intensity. Sierra determined (using the Rossi-Forel intensity scale) intensities of 9–10 between 27°S and 30°S (Willis, 1929). Intensities appeared to vary greatly depending on the site, with marshy fill having higher intensities than gravel terraces. Willis (1929) concluded that the length of significant damage was 500 km along the coast and at least 100 km inland. Significant damage occurred form sea level to over 3000 m in elevation. The low population density inland made it difficult to determine how far inland significant shaking occurred. Willis (1929) found that the towns of La Serena, Vallenar, and Copiapo were the most severely damaged by the 1922 earthquake (Figs 3 and 5).

Residents of most of the towns along the coast reported at least two and more commonly three shocks within the first few minutes of the 1922 earthquake (Willis, 1929). Residents of Coquimbo reported feeling two major shocks 1 minute apart, with the second shock shorter but sharper. Residents of La Serena felt three shocks in the first several minutes. Residents of Vallenar, Freirina, Huasco, Chanaral, and Copiapo all reported feeling three distinct shocks in the first few minutes. Tsunami heights of 5, 7, and 9 m were reported at Copiapo, Caldera, and Chanaral, respectively (Willis, 1929; Lockridge, 1985). Willis (1929) concluded that the 1922 earthquake was probably three earthquakes with different epicenters, hence the reason for the large, complex intensity pattern and the difficulty in locating the event. This is exactly what we find analyzing the *P* waveform—three subevents occurred in the first 75 s. It seems likely that the local resident did feel the three subevents as three separate shocks.

On December 4, 1918, a damaging earthquake shook Copiapo, completely destroying 20% of the houses and seriously damaging another 21% (Fig. 3) (Willis, 1929). The 1918 event was felt in Vallenar, but there was little damage. The town of Caldera was damaged by a tsunami with an estimated height of 5 m (Willis, 1929). The 1918 earthquake is located north of but adjacent to the estimated rupture area of the 1922 earthquake and has a $M_s = 7.6$ (Abe, 1981). This 1918 earthquake has an estimated rupture area much smaller than the 1922 event (Kelleher, 1972).

Previous earthquakes in the 1922 zone

The towns of La Serena, Vallenar, Coquimbo, and Copiapo were significantly damaged during the 1922 earthquake. These towns were settled early (in the early 1600 s) and provide an important source of information about many previous earthquakes along this segment of the Chile coast. Willis (1929) summarized the historic earthquake record for this segment of the chile coast and we will only briefly review it. The historic earthquake record starts in 1604 when an earthquake destroyed the church in La Serena. The town of Coquimbo was completely destroyed in 1648 by a devastating earthquake. La Serena was again shaken by an earthquake in 1792. It is difficult to evaluate the size of these earthquakes or even to guess if they are equivalent to the 1922 earthquake. In light of the absence of tsunami reports, we hesitate to suggest that any of these events were plate-rupturing events and equivalent to the 1922 earthquake.

On March 30, 1796, an earthquake struck Copiapo and La Serena, resulting in the toppling of the church tower, three deaths, and many injured. A few months later, on August 24, another earthquake struck with a longer duration but less force. There was no report of a tsunami for these 1796 earthquakes. In 1819 there were a series of three earthquakes on April 3, 4, and 11. These earthquakes severely damaged the towns of Copiapo and Vallenar. The reports suggest long-duration events with many aftershocks. A tsunami reached inland about 600 m (Willis, 1929; Heck, 1947). We speculate that this sequence in 1796 and 1819 may be equivalent to the 1918 and 1922 sequence (Fig. 2).

There were reports of moderate earthquakes in 1822, 1843, 1847, 1849, 1857, 1859, and 1864 along the 1922 segment (Fig. 2). But the descriptions of these earthquakes suggest that they were not nearly as large as the 1796, 1819, 1918 and 1922 earthquakes.

What stands out in the historic earthquake record is the clustering of large events in 1796 and 1819. In 23 years, five damaging events occurred along the same segment of the coast as the 1918 and 1922 earthquakes. The occurrence of the 1918 earthquake followed 4 years later by the 1922 earthquake cannot be overlooked. Although the 1918 earthquake was much smaller than the 1922 it was still very damaging. It seems quite possible that the multiple-pulse nature of the 1922 earthquake may have failed in smaller single events between 1796 and 1819. If this is the case, then this segment of the plate boundary is capable of extreme variations in the earthquake rupture mode between successive earthquake cycles. No characteristic earthquake occurs along this segment of the plate boundary, but rather a clustering events appears to occur over several years to several decades. This portion of the plate boundary may consist of small to moderate-size asperities that can fail individually as single earthquakes or together, generating a 1922-type rupture. Although we cannot predict what type of rupture mode will occur, it seems likely that when one asperity breaks, it loads an adjacent one, hence the temporal clustering of events.

The northern part of the 1922 rupture zone was the site of a $M_s = 7.5$ earthquake on October 4, 1983 (Fig. 2). This earthquake killed 5 people and caused damage in Copiapo. There was a minor tsunami reported and a maximum intensity of VII. The Harvard CMT is a thrust mechanism, with a depth of 38 km, and a seismic moment of 3.4×10^{20} Nm ($M_w = 7.8$) for this event (Dziewonski *et al.*, 1983).

APRIL 6, 1943 ILLAPEL EARTHQUAKE

The 1943 Illapel earthquake was well recorded teleseismically and the *P*-wave first motions are consistent with an underthrusting mechanism. All of the teleseismic *P*-wave records we obtained showed a compressional first arrival. Four *P* waveforms were modeled with an underthrusting focal mechanism and a fixed depth to determine the source time function. We used a grid search to step through a series of focal mechanisms at depths between 5 and 60 km in order to constrain these parameters and found that the teleseismic waveforms are not very sensitive to small variations in the focal mechanisms. The best fits to the data are for mechanisms with strikes between 330° and due north, shallow eastward dips and rakes between 80° and 100° (Fig. 7). However, for all the underthrusting mechanisms, the best depths are less than 35 km. For depths greater than 35 km, the fit of the synthetic to the observed seismogram is significantly degraded, and the source time function takes on a ringing characteristic, indicative of overestimating the depth (Christensen and Ruff, 1985). The resultant source time function has a single pulse of moment release with a duration of 24–28 s (Fig. 7a). We estimate a seismic moment of 6×10^{20} Nm ($M_w = 7.9$) for this event using the undiffracted *P*-waves. The 1943 earthquake is much smaller and simpler than the adjacent 1922 earthquake.

The Illapel earthquake had an aftershock zone of 360 km based on the S–P times of aftershocks recorded at La Paz, Bolivia (Kelleher, 1972). Four aftershocks

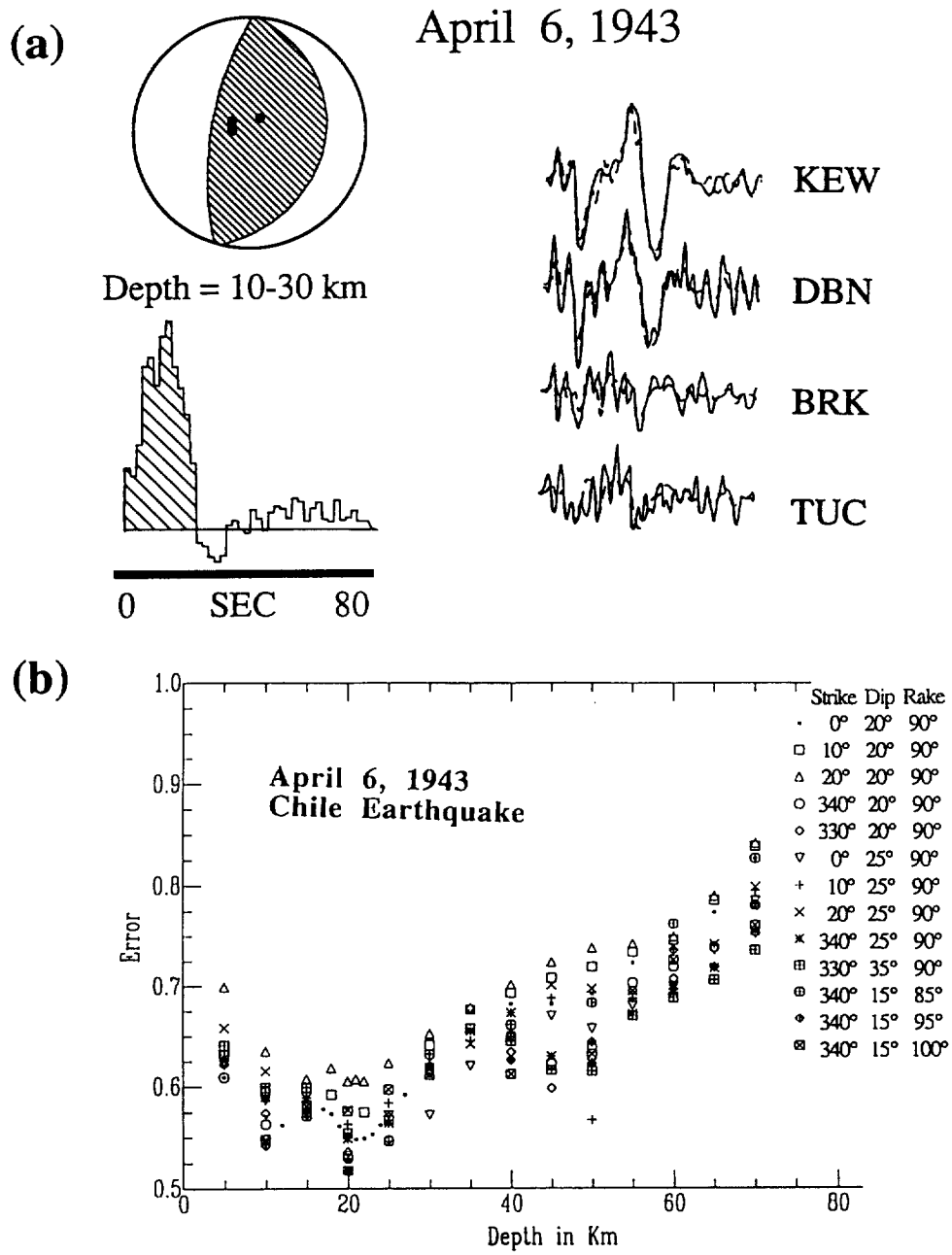

Fig. 7. (a) *P*-wave modeling results for the 1943 Illapel earthquake. Our preferred focal mechanism, source time function, and observed *P*-waves (solid lines) and sythetics *P*-waves (dashed lines) are shown. (b) An example of error versus depth from our grid search for different assumed focal mechanisms. For all these underthrusting mechanisms a depth of 10 to 30 km yields the best fit to the data.

were teleseismically relocated by Kelleher (1972). This event produced a local tsunami of 4–5 m and a far field tsunami in Japan of 10–30 cm (Lomnitz, 1971; Hatori, 1968). At Hanasaki, Japan the tsunami height for the 1922 and 1943 events were 60 and 10 cm, respectively, while at Kushimoto they were 70 and 25 cm, respectively (Hatori, 1968). An unpublished intensity map done by F. Greve in 1946 and described by Kelleher (1972) report high intensities (equivalent to 9–10 intensities on the Mercalli-Sieberg scale) between 30°S and 32.2°S. Previous earthquakes that appear to have ruptured this segment were on August 15, 1880, July 8, 1730, and possibly on May 13, 1647 suggesting recurrence intervals of 63, 150, and 63 years (Fig. 2) (Kelleher, 1972; Lomnitz, 1971). These last two events (1730 and 1647) are much larger than the 1943 earthquake and clearly ruptured the segment to the south and may have ruptured north into the 1943 zone.

DECEMBER 1, 1938 TALCA EARTHQUAKE

Along the south central segment of the Chile subduction zone the December 1, 1928 earthquake devastated the towns of Talca and Constitucion and killed

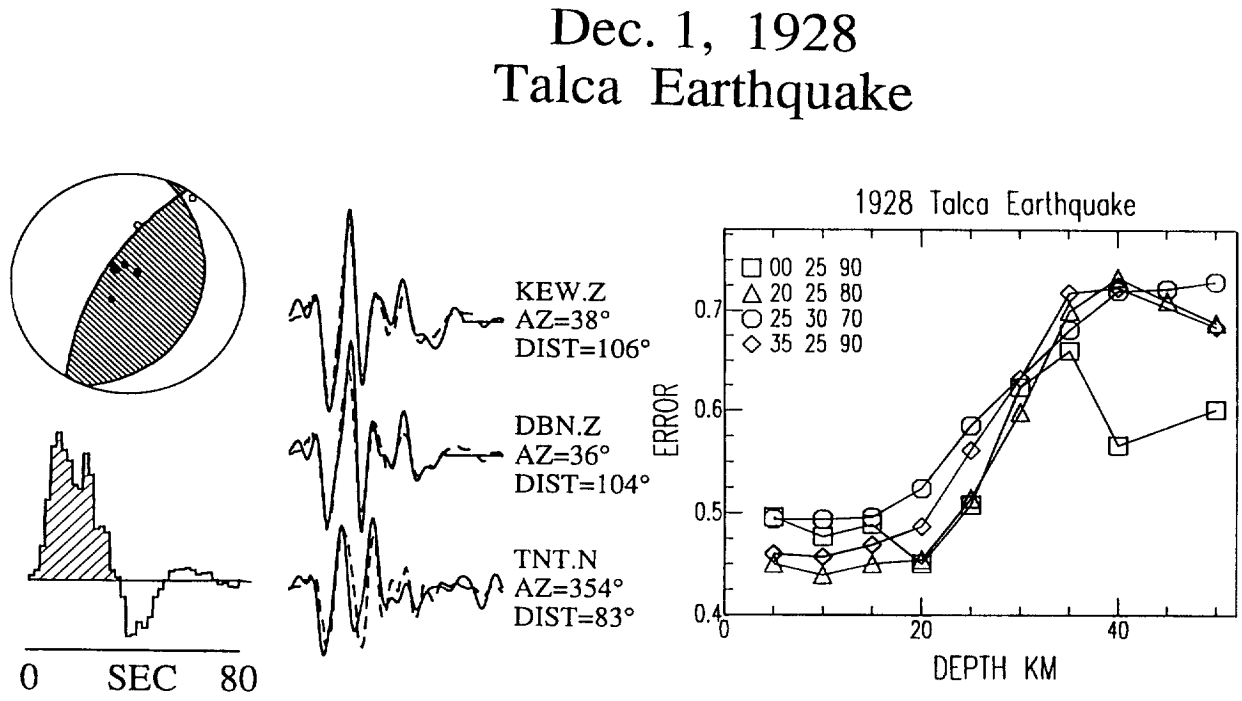

Fig. 8. *P*-wave modeling results for the 1928 Talca earthquake. Our preferred focal mechanism with *P*-wave first motions (upper left), source time function (lower left) and observed P waveforms (solid lines) and synthetic waveforms (dashed lines) are shown. On the far right shows an example of the errors for four different focal mechanisms as a function of depth. For these underthrusting mechanisms the best depths are less than 25 km.

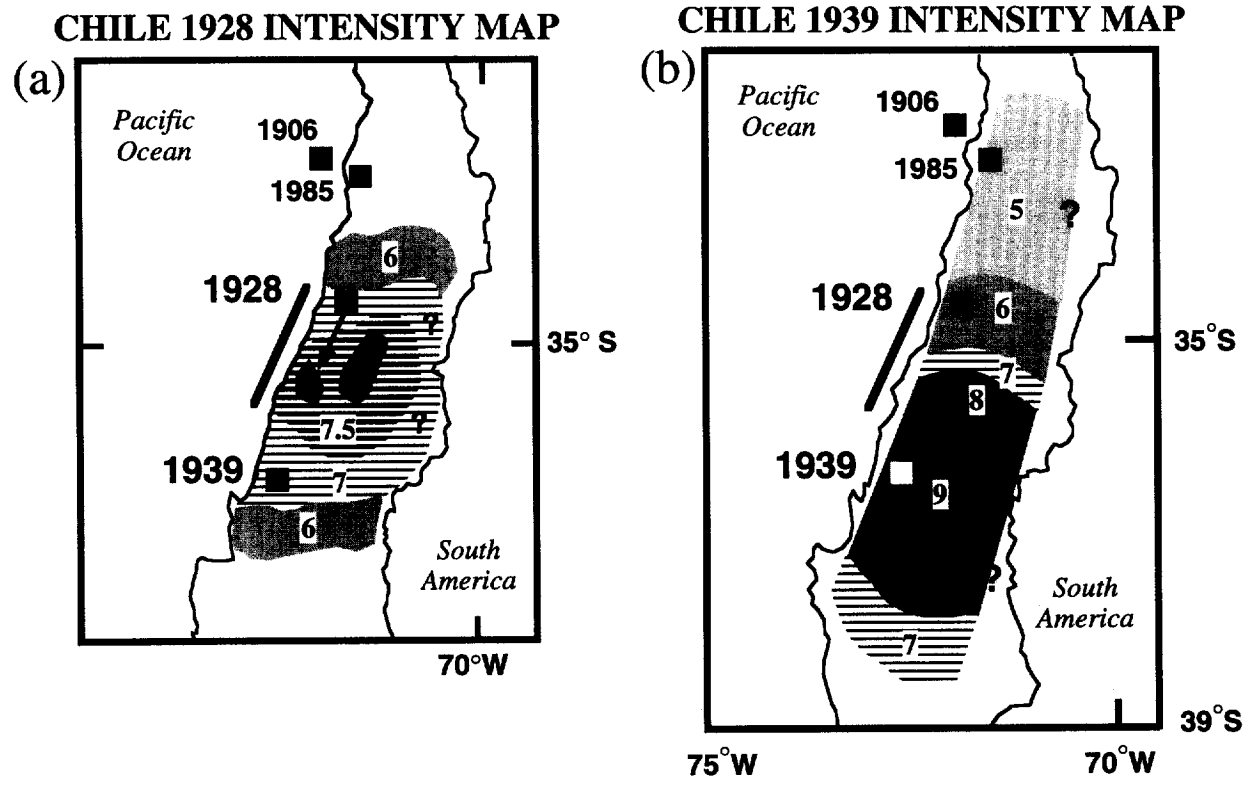

Fig. 9. (a) Contour map of intensities for the 1928 earthquake (M. Reyes, 1993). Notice the small area with maximum intensity 8. The solid bar represents our estimate of the rupture length of the 1928 earthquake. (b) Intensity contour map for the 1939 earthquake (M. Reyes, 1993). Notice the large area with maximum intensity 9 that occurs inland from the coast. The solid bar represents our estimate of the rupture of the 1928 earthquake.

over 200 people (Fig. 3). This event produced a local tsunami height of 1.5 m (Lomnitz, 1971). The long-period *P* waveforms for the December 1, 1928 earthquake are relatively simple (Fig. 8). The *P*-wave first motions constrain a steep nodal plane but not the shallow nodal plane. This combined with the tsunami strongly suggests an underthrusting focal mechanism for the 1928 earthquake. *P*-waves from stations KEW, DBN and TNT were recorded on long-period instruments and were used to investigate the focal mechanism, source time function, and depth. The focal mechanism and depth were fixed and then the waveforms were inverted simultaneously for a source time function using an omnilinear inversion scheme (Ruff 1989). We step through a range of focal mechanisms and depths to determine the best estimate of each. The *P*-waves recorded at KEW, DBN, and TNT have take-off angles near the center of the focal sphere and hence, are not very sensitive to small changes in the focal mechanism. Both *P*-wave first motions and the waveform modeling suggest an underthrusting focal mechanism with a strike near parallel to the trench and a shallow dip of 20°–30° to the east. Figure 8 shows the source time function determined from an inversion of three *P* waves using an underthrusting mechanism and a depth of 20 km. The source time function is simple with one main pulse of seismic moment release and a duration of 28 s. Figure 8 shows the result of multiple inversions at different depths using several acceptable focal

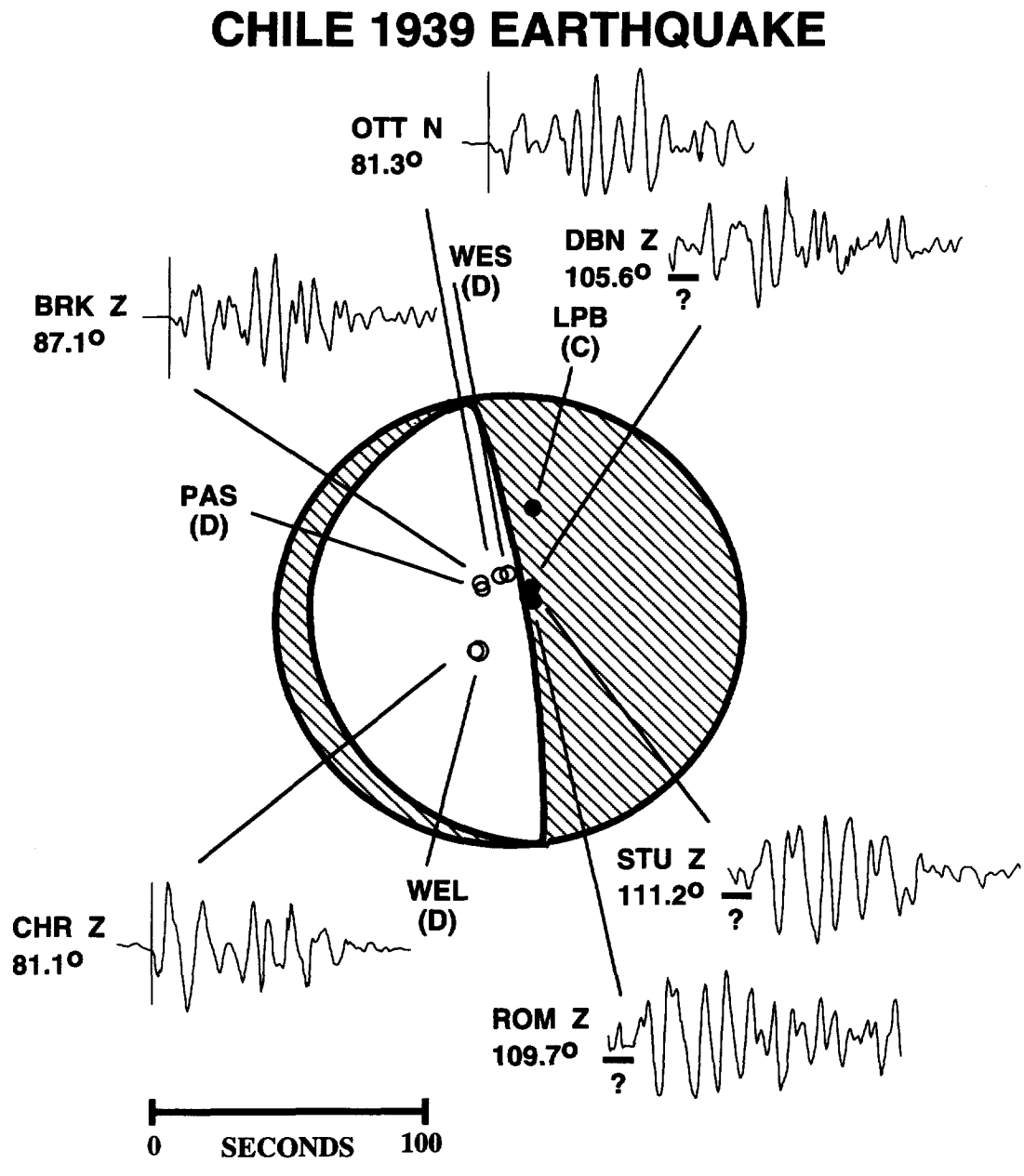

Fig. 10. *P*-wave first motion focal mechanism and waveforms for the 1939 earthquake. The shallow plane is completely unconstrained from the first motions. Note the difficulty in picking the first motions at stations in Europe (ROM, STU and DBN).

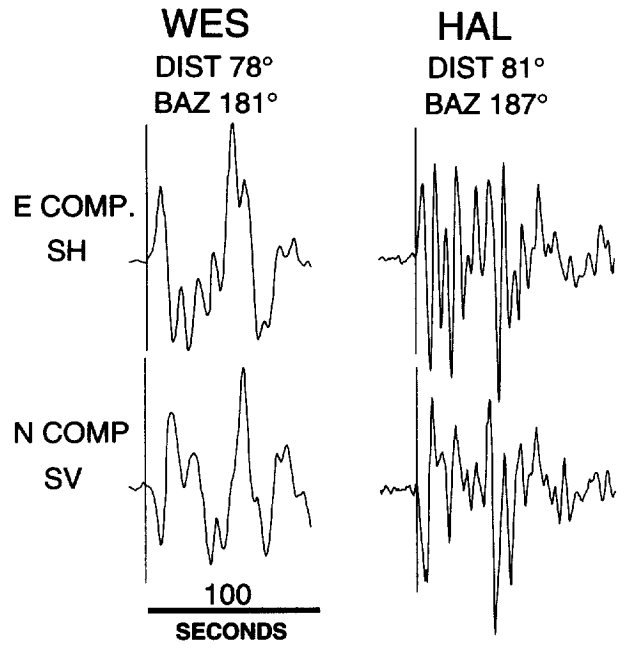

Fig. 11. Plot of the SH and SV components recorded at WES and HAL for the 1939 earthquake. The *S* waveforms are naturally rotated at WES.

mechanisms. The lowest errors (the best fit to the observed data) occur for depths of less than 25 km. We conclude that the 1928 earthquake is a shallow underthrusting event.

The seismic moment determined from the *P* waves ranges from 3 to 6×10^{20} Nm ($M_w = 7.9$). This is slightly smaller than the previous estimate of 8.0 (Abe, 1981). Reyes (1993, unpublished) reevaluated the seismic intensities for the 1928 event and found a north–south elongated area of maximum intensities (Mercalli-Sieberg scale) rather than an east–west pattern (Fig. 9a). The initial east–west pattern of high intensities reported by Bobillier (1929) was in part due to a volcanic eruption in the Andes on the same day. the highest intensities occur south of the 1928 epicenter, suggesting that at least part of the rupture was to the south. The 28 s duration and a range of rupture velocities between 2 and 3 km/s indicates that the 1938 earthquake probably ruptured (with high moment release) between 50 to 90 km from the epicenter in a direction primarily to the south. If it ruptured further south it did so with low seismic moment release. The S–P times for aftershocks recorded at La Paz, Bolivia indicate that all the aftershocks are south of the mainshock and correspond to a north–south area of 150 km (Kelleher, 1972). The southern rupture extent of the 1928 earthquake is probably north of the highest intensities reported for the adjacent 1939 earthquake zone (Fig. 9) as discussed in the next section. The northern rupture extent of the 1928 earthquake is difficult to determine but we find no indication of northward rupture. This event probably did not rupture into the southern end of the 1906 zone. In summary, the 1928 Talca earthquake is a shallow (less than 30 km) underthrusting event that probably ruptured < 150 km of the plate interface.

JANUARY 25, 1939 CHILLAN EARTHQUAKE

The most damaging earthquake in south central Chile this century occurred on January 25, 1939 (local Chilean date and time January 24, 1994, 11:32 p.m.). The 1939 earthquake caused 28,000 deaths and produced extensive damage to the city of Chillan (Saita, 1940; Sarasola, 1839). The major damage was confined to the Central Valley between Linares (35.8°S) and Los Angles (37.5°S) (Fig. 3) (Lomnitz, 1971). The *P*-waves for this event have a long duration and are more complex than those recorded for the 1928 event (Figs 4 and 10). There is a small amplitude precursor observed at some stations but at other stations this precursor is probably in the noise, hence, it is difficult to be sure we are picking the same onset at each station. Although the event was recorded in Europe, the *P*-waves do not have clear first arrivals that can be picked with confidence. The European stations are probably near nodal. If this is the case then the *P*-wave first motions suggest one nodal plane is steep but do not constrain the other nodal plane (Fig. 10).

In order to help constrain the focal mechanism we have employed a grid search for possible mechanisms using the SH/SV amplitude ratio and polarity observed at WES (Weston Observatory). The backazimuth from WES to the earthquake is 181°, hence, the *S* waves are naturally rotated to SH and SV waves (Fig. 11). The SH and SV waveforms also have a long duration and at this distance the *S* wave window is short because other phases (ScS, SkS) arrive before the *S* waves end. However, both the SH and SV have large impulsive first arrivals with opposite polarities at WES. At WES the ratio of the initial pulse of the SH to SV is 1.25 with SH polarity up (east) and the SV polarity down (south). As a check we also looked at *S* waves recorded at HAL (backazimuth 187°). At HAL the ratio of SH to SV is 0.9 with SH polarity up (east) and the SV polarity down (south). For our grid search we calculated synthetic SH and SV waveforms for the station geometry and instrument response at WES for a large range in strike, dip and rake. we then determined the synthetic SH and SV amplitude ratio of the initial pulse and compared it to the observed value. Most of the focal mechanisms that produce the correct ratio do not have the correct polarities of both SH and SV and hence, can be eliminated. In general a strike of 320° to 350°, a dip of 60° to 80° to the east and a rake of −90° to −130° have the appropriate SH/SV ratio and polarity and the correct *P*-wave polarity.

The combination of our grid search and the *P*-wave first motions indicate that the 1939 earthquake is not an underthrusting event but rather a normal fault

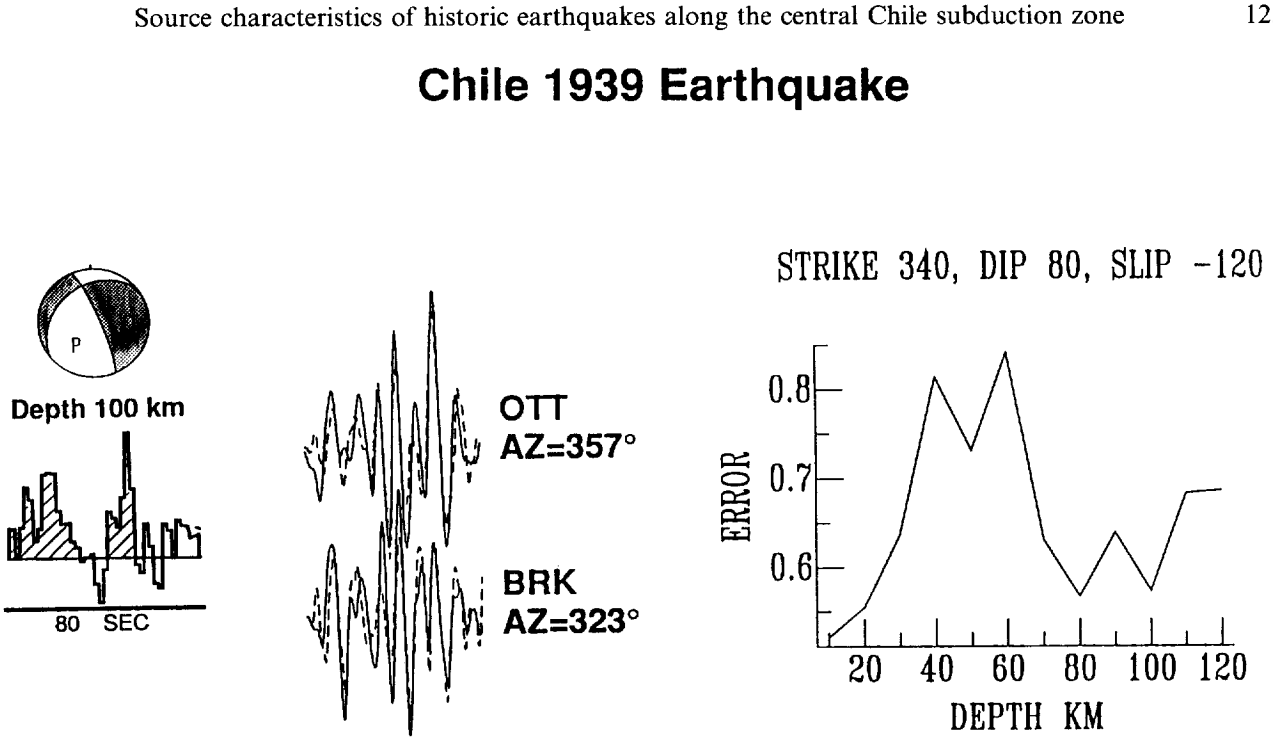

Fig. 12. *P* waveform modeling results of the 1939 Chillan earthquake. Our preferred focal mechanism (upper left), source time function (lower left), observed *P* waveforms (solid lines) and synthetic waveforms (dashed lines) are shown. On the far right shows an example of the errors as a function of depth.

earthquake. The depth is more problematic due to the complex trade-off between depth and the source time function. We fix the focal mechanism and invert the data at a series of fixed depths for the source time function using *P*-waves recorded at BRK and OTT. We use BRK and OTT because they are not nodal and have clear first arrivals. this is a very limited azimuth range, hence, we must not over interpret the results. The results suggest two possible depths, a very shallow depth (around 10 km), or a depth between 80 and 100 km (Fig. 12). This uncertainty is due to the trade-off between depth and source time function. The deeper depth suggests that the event is in the downgoing slab while the shallow depth suggests the event is in the overriding continental crust. Although we prefer the deeper depth, it is difficult to rule out a very shallow source depth from the waveforms alone. There are nor reports of surface rupture and we would expect a $M_s = 7.8$ ($m_b = 7.6$) (Abe, 1981) earthquake in the upper curst to rupture the surface. The source time function for the 1939 earthquake is also complex. For our preferred depth of 80 to 100 km the source time function has two pulses of moment release. The first pulse has a duration of approximately 25 s followed by a second pulse starting 40 s later with a duration of approximately 20 s. This model also fits the *P* wave at CHR allowing for some directivity but it is still difficult to model the waveforms recorded at stations in Europe (DBN, STU and ROM) with this model. Part of the problem may be the nodal character of these records but we cannot rule out a more complicated rupture with a change in focal mechanism and or depth for each pulse of moment release.

The Mercalli-Sieberg intensities for the 1939 earthquake are shown in Fig. 9b (M. Reyes unpublished, 1993). The zone of maximum intensity 9–10 covers a large area and occurs inland of the coast in the Central Valley. There was no report of a tsunami associated with the 1939 earthquake. All the available evidence indicates the 1939 earthquake is clearly not an underthrusting event but rather a normal fault event.

We have looked at the geometry of the subducted slab in the region of the 1939 earthquake to see if our depth of 80–100 km for the 1939 earthquake is consistent with the event occurring in the down-going slab. The epicenter for the 1939 event is about 220 km inland from the trench but probably is not well constrained in the east–west direction. Seismicity between 37°S–38°S degrees shows a poorly defined slab but suggests that the slab occurs at a depth of 60–80 km at a location 220 km landward from the trench (Ficuentes, 1989; Kadinsky-Cade, 1985; Chaill and Isacks, 1992). Given the uncertainty of the 1939 location it seems reasonable that this event could have occurred in the downgoing slab.

Moderate sized intermediate-depth normal fault earthquakes with mechanisms similar to our preferred mechanism for the 1939 earthquake are relatively common in the down going slab along the coast of

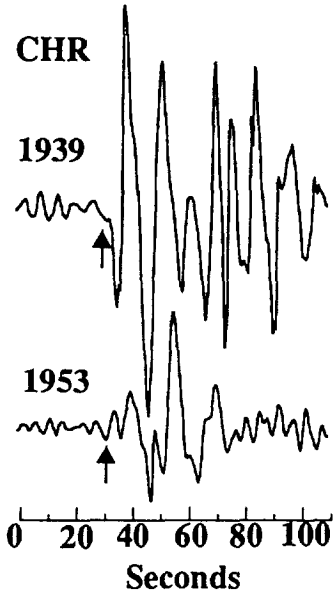

Fig. 13. Plot of *P* waveforms recorded at CHR for the 1939 (Dist = 81.2°) and the 1953 (Dist = 80.5°) earthquakes. The *P* waveforms are plotted with a 30 s noise window before the first arrival as indicated by the arrows. The 1939 event has a dilitational first motion and the 1953 event has a more nodal but compressional first motion.

Chile. Malgrange and Madariaga (1983) and Malgrange et al. (1981) documented intraplate down-dip extensional earthquakes within the slab ($M > 6$) between 20°S and 33°S. Cahill and Isacks (1992) compiled focal mechanisms for intermediate-depth events between 33°S and 37°S and find down-dip tension consistent with our preferred focal mechanism for the 1939 earthquake. Astiz (1987) determined a normal fault focal mechanism and a depth of 120 km for an event on March 1, 1934, ($M_s = 7.1$) located just south of the 1939 event. To the north near 24°S a large normal fault event occurred on December 9, 1950 ($m_b = 7.7$) at a depth of 100 km (Campos, 1989; Abe, 1981). Intermediate depth normal fault earthquakes along this segment of the Chile subduction zone are fairly common. Astiz (1987) has pointed out that in a strongly coupled subduction zone such as Chile we might expect to see normal fault events at the down-dip edge of the coupled zone, particularly before a large underthrusting event. In light of this interpretation of normal fault events being down-dip of coupled subduction zones we investigated the coupling of the interplate zone up-dip from the 1939 earthquake. In particular, to determine when was the last earthquake to rupture the up-dip segment.

Relative relocation of the 1928 and 1939 earthquakes

A possible scenario is that the 1928 earthquake ruptured into the up dip region of the 1939 earthquake. Earthquake locations are often difficult for historic earthquakes in South America due to the poor station distribution. In particular, the location in the east–west direction is poorly constrained. The locations we have used in this study were determined by the ISC in 1985 and differ slightly from the original ISS locations. These locations suggest that the 1928 earthquake was north of the 1939 event and our study shows that the 1928 earthquake was probably not large enough to have ruptured the entire underthrusting zone trenchward of the 1939 event. As a check we did a relocation of the 1928 earthquake relative to the 1939 event. We used the difference in travel times between 26 stations that recorded both events and reported the times to the ISS bulletin. We fixed the depths of both events at 20 km and 80 km for the 1928 and 1939 events, respectively. We find that the 1928 event is located 246 ± 45 km north of the 1939 earthquake. Although the errors are still large this suggests that the 1928 earthquake did not occur trenchward of the 1939 event.

May 6, 1953 Chile earthquake

The May 6, 1953 earthquake ($M_s = 7.6$), although much smaller, occurred in the vicinity of the 1939 earthquake and has a similar but less damaging intensity pattern. There were no reports of a tsunami for the 1953 earthquake (Askew and Algermissen, 1985; Lomnitz, 1971). Hence, it is important to determine if

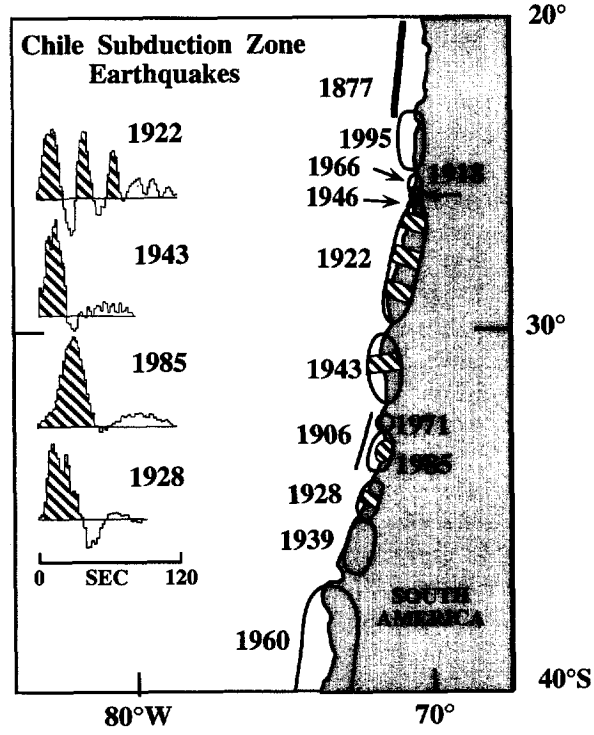

Fig. 14. Summary of source time functions for underthrusting earthquakes along the Chile coast. The time scale is the same but each source time function is plotted at the same amplitude. shown in map view are the aftershock areas and schematic regions of concentrated moment release for each earthquake.

the 1953 event recorded at PAS, STU, and ROM have clear compressional first motions. Figure 13 shows a comparison of *P* waveforms recorded at CHR for both the 1939 and 1953 earthquakes. The first motion for the 1939 event is clearly dilitational while the first motion for the 1953 earthquake is probably compressional. The *P*-wave first motions suggest a thrust or reverse fault for the 1953 event rather than a normal fault. The *P*-wave first motions are not the same as the 1939 earthquake, hence, the 1953 earthquake probably has a different mechanism.

The highest intensities were also inland in the Central Valley for the 1953 earthquake similar in location to the 1939 event but the overall intensities and damage were much less. The similar intensity pattern is probably a result of the local site amplifications in the Central Valley and not due to similar sources.

SEGMENTATION ALONG THE CENTRAL CHILE SUBDUCTION ZONE

The segmentation of the central Chile subduction zone is difficult due to the large variation in earthquake size and rupture length of the events. Segmentation has generally been defined by the largest earthquakes to occur this century but several studies have shown that the earthquake size changes between successive cycles and this century's seismicity may not be representative of past events (Swenson and Beck, 1996; Beck and Nishenko, 1990). Even so there are some interesting observations for several segments along the Chile coast. Figure 14 shows a summary of the source time functions and rupture areas for the underthrusting earthquakes along the coast of Chile this century.

Segment 26°S to 32°S

The 1922 segment failed in a multiple asperity type rupture (Fig. 14). The historic record suggests that this region has clusters of events indicating a very heterogeneous style of faulting (Fig. 2). Two earthquakes in 1796 (March 30 and August 24) and three earthquakes in 1819 (April 3, 4 and 11) probably ruptured the 1922 segment. This clustering of events in time suggest that after one large earthquake the region will not necessarily be seismically quiet. In contrast, to the south the 1943 zone failed in a single small asperity (within a large aftershock area) (Fig. 14). The historic record does not show clustering of events. The previous earthquake along the 1943 segment was a well documented event on August 15, 1880 (Fig. 2) (Lomnitz, 1971). It is possible that the July 8, 1730 and May 13, 1647 earthquakes ruptured as far north as this segment (Nishenko, 1985). the available data for the 1943 zones suggests a much less heterogeneous type of rupture than the 1922 zone (Fig. 14).

Segment 32°S to 34°S

Although this segment is not the focus of this study it is interesting to compare the earthquake record to the other regions to the north and south. This segment of the subduction zone has failed in large underthrusting earthquakes on December 16, 1575, May 13, 1647, July 8, 1730, November 19, 1822, August 16, 1906 and March 3, 1985 (Fig. 2). This sequence gives a recurrence period of 80 ± 9 years for the 1985 zone (Comte *et al.*, 1986). This is a strikingly tight recurrence interval given that the size and rupture lengths of these events varied between cycles. the most recent of these events, the 1985 earthquake had a simple source time function with one pulse of moment release (Christensen and Ruff, 1986) much like the 1943 and 1928 earthquakes (Fig. 14).

Segment 34°S to 37.5°S

The 1939 earthquake is an intraplate event and probably occurs within the down-going slab. The 1928 earthquake probably did not rupture the interplate contact zone up-dip from the 1939 earthquake. An important question is then, what is the nature of this segment of the plate boundary up-dip from the 1939 event, and when did it last fail? As discussed previously the 1953 ($M_s = 7.6$) earthquake is probably not a normal fault event and could be an underthrusting event that ruptured a small segment of the plate boundary. There are two possible scenarios. First, the 1928 and 1953 events ruptured the entire region between the 1906 event to the north and the 1960 earthquake to the south, hence, there is no seismic gap. Second, the 1928 ruptured a segment north of the up-dip region of the 1939 event and the 1953 earthquake was either an intraplate event or too small to rupture the remaining segment and is probably not equivalent to previous historic underthrusting earthquakes in this region. In this case there is an important seismic gap (Barrientos, 1990). The historic earthquake record suggests that this segment of the plate boundary failed in very damaging underthrusting events on February 20, 1835, May 25, 1751, and probably March 15, 1657 (Fig. 2) (Lomnitz, 1971; Silgado, 1985). These events all produced tsunamis and had high intensity reports along the coast of Chile between 36°S and 38°S. In light of this information, we would categorize this segment of the Chilean subduction zone as a possible seismic "gap" that requires further study. The plate convergence rate is approximately 9 cm/yr and the time since the last underthrusting event is 158 years (assuming the 1953 event was too small to completely fill the gap). This would suggest a very large amount of accumulated

tectonic slip (14 m) if the plate boundary has been locked since 1835.

CONCLUSIONS

We have analyzed waveforms for historic earthquakes along the central Chile subduction zone. we find that the following earthquakes are shallow underthrusting events with decreasing size; 1922, 1943, and 1928. We find that the 1922 Atacama earthquake had a complex source with a duration of 75 s and at least 3 pulses of moment release. The historic earthquake record suggests that the 1922 segment tends to fail in multiple events clustered in time. The adjacent 1943 Illapel earthquake is much simpler with a duration of 24 s and one pulse of moment release. The 1928 Talca earthquake had a duration of 28 s and one pulse of moment release. The intensities and aftershock locations suggest a unilateral rupture to the south for the 1928 earthquake. The 1922 earthquake had a heterogeneous rupture while the 1943 and 1928 events had very simple ruptures. The 1939 Chillan earthquake was not an underthrusting but rather a complex normal fault earthquake. Our preferred model is a normal fault mechanism at a depth of 80 to 100 km with two pulses of moment release and a total duration of approximately 60 s. The 1939 earthquake was clearly more destructive than the other similar size or larger events. This may in part be due to the intraplate nature of the event but also due to high amplification of the sites in the Central Valley of south central Chile. The previously documented underthrusting earthquake to rupture the underthrusting region up-dip from the 1939 earthquake was in 1835. This suggests that this region of the plate boundary between about 36°S and 37.5°S is a seismic gap that could produce a damaging earthquake.

Acknowledgements — We thank all the seismic station operators around the world who provided us with copies of the historic seismic records. We thank Jun Wu for help with the 1943 earthquake and Steve Myers and George Zandt for useful suggestions and comments. This study was funded by NSF grants EAR-931440 and EAR-9017358. SASO contribution ♯103.

REFERENCES

Abe, K. 1981. Magnitudes of large shallow earthquakes from 1904 to 1980. *Phys. Earth Planet. Inter.* **27**, 72–92.

Abe, K., and Noguchi, S. 1983. Deteminations of magnitude for large shallow earthquakes 1897–1917. *Earth Planet. Inter.* **32**, 45–59.

Askew, B.L., and Algermissen, S.T. 1985. Catalog of earthquakes for South America: Hypocenter and intensity data *Ceresis publication* , 4–7c.

Astiz, L.M. 1987. Study of intermediate-depth earthquakes and interplate seismic coupling. PhD dissertation. California Institute of Technology.

Barrientos, S. 1990. Is the Pichilemu-Talcahunao (Chile) region a seismic gap? *Seism. Res. Letters* **61**, 43.

Beck, S., and Nishenko, S. 1990. Variations in the mode of great earthquake rupture along the central Peru subduction zone. *Geophys. Res. Lett.* **17**, 1969–1972.

Berninghausen, W.H. 1962. Tsunamis reported from the west coast of South America 1562–1960. *Bull. Seismo. Soc. Am.* **52**, 915–921.

Bobillier, C. 1930. Observiaciones de 1928 Terremoto Del de lo de Dicibre. *University de Chile* **No XX**, .

Cahill, T., and Isacks, B. 1992. Seismicity and shape of the subducted Nazca plate. *J. Geophys. Res.* **97**, 17,503–17,529.

Campos, J. 1989. Determinacion de parametros focales por medio de modelamiento de ondas de cuerpo del sismo de 9 de Dic. de 1950. In *Magister en cencias mencion geofisica.* Universidad de Chile, Santiago, Chile.

Campos, J., and Kausel, E. 1990. The large 1939 intraplate earthquake of southern Chile *Seism. Res. Letters* **61**, 43.

Christensen, D., and Ruff, L. 1985. Analysis of the trade-off between hypocentral depth and source time function. *Bull. Seismo. Soc. Am.* **75**, 1637–1656.

Christensen, D., and Ruff, L. 1986. Rupture process of the March 3, 1985 Chilean earthquake. *Geophys. Res. Let.* **13**, 721–724.

Comte, E., Eisenberg, A., Lorca, E., Pardo, M., Ponce, L., Saragoni, R., Singh, S., and Suarez, G. 1986. The 1985 central Chile earthquake, a repeat of previous earthquakes in the region? *Science* **233**, 449–453.

Dziewonski, A., Friedman, J., and Woodhouse, J. 1984. Centroid-moment tensor solutions for October–December 1983. *Phys. Earth Planet. Inter.* **34**, 129–136.

Hatori, T. 1968. Study of Distant tsunamis along the coast of Japan, Part 2, tsunamis of South American origin. *Bull. Earthquake Res. Inst.* **46**, 345–359.

Heck, N.H. 1947. List of seismic sea waves. *Bull. Seismo. Soc. Am.* **37**, 269–286.

Kadinsky-Cade, K. 1985. Seismotectonics of the Chile margin and the 1977 Caucete earthquake of western Argentina. Ph.D thesis. Cornell University, Ithaca, NY, 253 p.

Kelleher, J. 1972. Rupture zones of large South American earthquakes and some predictions. *J. Geophys. Res.* **77**, 2089–2103.

Lockridge, P. 1985. Tsunamis in Peru–Chile. In *Report SE-39*, 95 p. p. World Data Center A for Solid Earth Geophysics.

Lomnitz, C. 1971. Grandes Terremotos y Tsunamis en Chile Durante el Period 1535–1955. *Geofisica Panamericana* **1**(1), 151–178.

Malgrange, M., and Madariaga, R. 1983. Complex distribution of large thrust and normal fault earthquakes in the Chilean subduction zone. *Geophys. J. R. Astro. Soc.* **73**, 489–505.

Malgrange, M., Deschamps, A., and Madariaga, R. 1981. Thrust and extensional faulting under the Chilean coast: 1965, 1971 Aconcaua earthquakes. *Geophys. J. R. Astro. Soc.* **66**, 313–331.

Nishenko, S. 1985. Seismic potential for large and great interplate earthquakes along the Chilean and southern Peruvian margins of South America: a quantitative reappraisal. *J. Geophys. Res.* **90**, 3589–3615.

Nishenko, S. 1991. Circum-Pacific seismic potential 1989–1999. *Pure Appl. Geophys.* **135**, 169–259.

Ruff, L. 1989. Multi-trace deconvolution with unknown trace scale factors: Omnilinear inversion of *P* and *S* waves for source time functions. *Geophys. Res. Let.* **16**, 1043–1046.

Ruff, L.J., and Kanamori, H. 1983. The rupture process and asperity distribution of three great earthquakes from long-period diffracted *p*-waves. *Phys. Earth Planet. Inter.* **31**, 202–230.

Saita, T. 1940. The great Chilean earthquake of January 24, 1939, University Tokyo. *Bull. Earthq. Res. Inst.* **18**, 446.

Sarasola, S. 1939. Communication: The Chilean earthquake of January 25, 1939. *Bull. Seismo. Soc. Am.* **729**, 509–512.

Silgado, E. 1985. Destructive earthquakes of South America 1530–1894. *Center of Regional Seismology for South America, Ceresis* **10**, 315 p.

Swenson, J., and Beck, S. 1996. Source characteristics for the 1942 Ecuador and 1942 Peru subduction zone earthquakes. PAGEOPH **146**, 67–102.

Willis, B. 1929. *Studies in comparative seismology: Earthquake conditions in Chile*, 382. Carnegie Institution of Washington, Washington.